RECEIVED BY OSTI JUN 24 1985

BNL 36494
OG 839

CONF-8504133--4

BNL--36494

DE85 012179

International Conference on Hadron Spectroscopy
College Park, Maryland, April 20-22, 1985

PARTIAL WAVE ANALYSIS OF $K\bar{K}\pi$ SYSTEM IN THE D AND E/IOTA REGIONS

S.U. Chung, R. Fernow, H. Kirk, S.D. Protopopescu, D.P. Weygand
Brookhaven National Laboratory, Upton, New York 11983

D. Boehnlein, J.H. Goldman, V. Hagopian, D. Reeves
Florida State University, Tallahassee, Florida 32306

R. Crittenden, A. Dzierba, T. Marshall, S. Teige, D. Zieminska
Indiana University, Bloomington, Indiana 47401

Z. Bar-Yam, J. Dowd, H. Rudnicka, W. Kern
Southeastern Massachusetts University, N. Dartmouth, MA 02747

Presented by D. Zieminska

ABSTRACT

We have performed a partial-wave analysis of the $K^+\bar{K}^0\pi^-$ system produced in the reaction $\pi^- p \to K^+\bar{K}^0\pi^- n$ at 8.0 GeV/c. We find that the D(1285) is a $J^{PG} = 1^{++}$ state coupling predominantly to a $\delta\pi$ decay channel, while the E(1420) peak consists mostly of a $J^{PG} = 0^{-+}$ wave with a substantial $\delta\pi$ decay mode. There is little evidence of a 1^{++} resonance at the E mass.

A $J^{PC} = 0^{-+}$ state called the $\iota(1440)$ is considered to be a prime glueball candidate because it is produced prominently in J/ψ radiative decays[1] where $C = +1$ glueballs are expected to be copiously produced. However, this assertion rests on the premise that it is distinct from the E(1420) discovered earlier by Baillon et al[2] ($J^{PC} = 0^{-+}$ or 1^{++}) and later determined to be a 1^{++} state in a Dalitz-plot analysis of a separate experiment by Dionisi, et al.[3]. Since the spin-parity analysis of the E(1420) was based on limited statistics, it is desirable that a study of the spin-parity content of the E region be performed on a large-statistics sample.

Our study of the $K\bar{K}\pi$ system is based on about 10,000 events of the reaction

$$\pi^- p \to K^+ K^0_S \pi^- n \qquad (1)$$

MASTER

DISTRIBUTION OF THIS DOCUMENT IS UNLIMITED

at 8 GeV/c. The data come from our experiment performed with the BNL Multiparticle Spectrometer (MPS). The layout of the experiment is shown in Fig. 1. A tagged π^- beam at 8 GeV/c impinged on a 30 cm liquid-hydrogen target, located in the MPS magnet and surrounded on four sides by a lead-scintillator sandwich veto box (TB) for rejecting backward particles. Within the MPS magnet and downstream of the veto box were located 7 drift-chamber modules* with 7 measuring planes each, interspersed with three proportional wire chambers (P1, P2 and P3). In addition, a high-pressure Cherenkov counter hodoscope (C1) with γ-threshold = 10 and two scintillation-counter hodoscopes (H1 and H2) were placed downstream of the MPS magnet.

The trigger required two charged particles traversing the first PWC (P1 = 2), no particles entering the target veto box ($\overline{TB}$), a multiplicity increase to four at the second PWC (P2 = 4), a forward-going positive particle traversing C1, H1 and H2 with momentum $p \geq 1.5$ GeV/c (as measured on-line by P2, P3, and H2), and its identification as a K^+ (or proton) using $\overline{C1}$ and H1 ($H1 \cdot \overline{C1}$). The on-line detection of K^+ (or proton) was made through the so-called RAM-trigger, a three-dimensional (128 x 128 x 128) coincidence matrix system using random-access memories. The trigger actually required a coincidence of two RAM's; P2 x P3 x H2 for momentum selection and P2 x P3 x $H1 \cdot \overline{C1}$ for non-pion identification. A total of 1.5 x 10^6 triggers was recorded in a 200-hour run at the AGS in Spring 1983, yielding 55,000 events that satisfied a two-prong + V^0 topology.

Fig. 2a shows the missing-mass squared distribution, and Fig. 2b shows the $\pi^+\pi^-$ spectrum for the decay vertex. They demonstrate that our data have good mass resolution, no systematic bias, and little contamination from other reactions. The $K^+K^0_S\pi^-$ spectrum in Fig. 2c for reaction (1), from a sample of 16,000 events after cuts on K_S mass, n mass and $t < 1.0$ GeV^2, is dominated by peaks at the D(1285) and the E(1420) masses. A fit to the spectrum in Fig. 2c with two simple Breit-Wigner functions and a polynomial background gives m = 1285 ± 2 MeV and Γ = 22 ± 2 MeV for the D(1285) and m = 1421 ± 2 and Γ = 60 ± 10 MeV for the E(1420). Our estimate of the mass resolution is less than 7 MeV in the E region. Dalitz plot distribution for the $K^+K^0_S\pi^-$ system in the E region, $1.37 < M(K^+\overline{K}^0\pi^-) < 1.49$ GeV, and above the E region, $1.49 < M(K^+\overline{K}^0\pi^-) < 1.60$ GeV, is shown in Fig. 3.

Results of a Dalitz-plot analysis with Zemach amplitudes[5] were reported last summer in Leipzig[6]. Below we present results of the complete partial wave analysis of the same data. As before, we discuss the $K\bar{K}\pi$ final state in terms of an isobar model, i.e. we treat it as a superposition of quasi two-body states: $\delta\pi$ and $K^*(890)\bar{K}$. The decay $\delta \to K\bar{K}$ was parametrized by a two-channel form as given by Flatte[7] and $K^* \to K\pi$ was parametrized by the conventional p-wave Breit Wigner form. For a given $K\bar{K}\pi$ mass we define the amplitude in terms of reflectivity states $a = (J^{PG}M^{\eta}$ (isobar)), where J is the spin, P is the parity, G is the G-parity, M is the third component of the spin in the Gottfried-Jackson frame, η is the eigenvalue of the reflection operator in the production plane and (isobar) is the isobar state, K^* or δ. We make the factorization assumption, namely, that the $J^P(\delta)$ and $J^P(K^*)$ states have the same density matrix, only different couplings to the final state. The reflectivity amplitues depend on five variables: three Euler angles which rotate from the Gottfried-Jackson system to the Dalitz system and two Dalitz-plot variables.

For reaction (1), where the recoiling baryon is a spin 1/2 particle, the density matrix is constrained to have rank ≤ 2. It can be written in the form[8]:

$$\rho_{aa'} = \sum_{k=1,2} V_{ak} \cdot V_{a'k} \qquad (2)$$

where V_{11} and V_{22} are real positive and the rest are complex numbers. This parametrization ensures that all the constraints for the physical density matrix are satisfied and the fitting procedure involves a minimum number of parameters for a given set of states considered.

For the $K\bar{K}\pi$ system from threshold to 1.6 GeV it is found that the states $J^{PG} = 0^{-+}, 1^{++}, 1^{+-}, 1^{-+}$, with all allowed M^{η} values and incoherent background are sufficient to describe the data.

For the states $J^{PG} = 0^{-+}$ and 1^{++}, both $\delta\pi$ and K^*K decay modes are allowed, while for 1^{+-} and 1^{-+} only the $K^*\bar{K}$ decay mode is allowed. A 1^{++} state can couple to the final state $K^*\bar{K}$ (or its charge conjugate) via S- or D-wave orbital angular momentum, but including only the S-wave was adequate to describe the data.

We have performed a maximum-likelihood analysis with the log of the likelihood given by

$$L = \sum_{i=1}^{n} \ln \frac{I(\tau_i)}{\int I(\tau)\, A(\tau) d\tau} \qquad (2)$$

where $I(\tau)$ is the full intensity distribution at the point τ and $A(\tau)$ represents the finite acceptance of our apparatus. The results are displayed in Fig. 4, where the different J^{PG} waves are given as functions of the $K\bar{K}\pi$ mass. It is seen that the 1^{++} wave is dominant at the D(1285) mass, confirming that it is a 1^{++} state.[9] Although the $\delta\pi$ decay mode is definitely dominant for the D, a considerable amount of $K^*\bar{K}$ decay mode can be accommodated interfering destructively with the $\delta\pi$ mode.

The behavior of the 0^{-+} wave at the E(1420) region shows clearly that the E peak seen in our data is mostly in a 0^{-+} state. In fact, we estimate that at least 70% of the E peak is attributable to the 0^{-+} wave. Analysis of the breakup of the 0^{-+} state into $\delta\pi$ and $K^*\bar{K}$ decay modes, (Fig. 5) indicates that the δ mode is predominant, but that the $K^*\bar{K}$ decay mode is definitely required, with strong constructive interference between them, to adequately describe the data. The 1^{++} state, (Fig. 4b), which is mainly $K^*\bar{K}$ with little $\delta\pi$, exhibits a sharp rise with the onset of the $K^*\bar{K}$ threshold at 1.4 GeV and levels off above the E peak.

The 1^{-+} wave (Fig. 4d) is slowly rising as $K\bar{K}\pi$ increases from $K^*\bar{K}$ threshold to 1.6 GeV. It is found to be produced predominantly in the $M^{\eta} = 0^-$ state, at small t, which is consistent with the $\rho(1600)$ production via a pion exchange. A moderate amount of background (Fig. 4e) is required above 1.4 GeV indicating the presence of states with spin 2 and higher, which are not included explicitly in this analysis.

The resonance interpretation of the 0^{-+} wave and nonresonant interpretation of 1^{++} and 1^{+-} waves is consistent with the measured phase differences as shown in Fig. 6. The relative phase of the $1^{++}0^+(K^*)$ and $1^{+-}0^+(K^*)$, (Fig. 6a), is slowly rising by about 90° over the $K\bar{K}\pi$ mass range studied, suggesting that either both or none of them are resonating in the E region. The phase difference between the 0^{-+} wave and the waves

$1^{+-}0^{+}(K^{*})$ and $1^{++}0^{+}(K^{*})$ is shown in Fig. 6c and 6d, respectively. Major features of the $K\bar{K}\pi$ mass dependence of these phase differences and of the 0^{-+} intensity may be understood in terms of the following parametrization: the 0^{-+} wave is represented by a Breit Wigner form with M = 1402 MeV and Γ = 47 MeV and a constant background with a phase of 90° relative to the resonance low-mass tail; the phase of the $1^{+-}0^{+}(K^{*})$ wave is assumed to be constant and that of $1^{++}0^{+}(K^{*})$ to be decreasing linearly with $K\bar{K}\pi$ mass. The results, represented by the dotted curves in Figs. 4a, 6a, 6c and 6d, are in qualitative agreement with the data.

We also studied the $K\bar{K}\pi$ production in $\bar{p}p$ annihilation at 6.6 GeV/c. In this case we required a change of topology from 2 or greater at P1 to 4 or greater at P2. We collected a total of 4 x 10^{6} triggers. The $K^{+}K^{o}_{S}\pi^{-}$ spectrum for the $\bar{p}$ beam is shown in Fig. 7. Both D and E mesons are observed, with mass and width m = 1282 ± 2 MeV, Γ = 27 ± 8 MeV for the D(1285) and m = 1416 ± 5, Γ = 80 ± 30 MeV for the E(1420). Fig. 8 shows results of te Dalitz plot analysis of the $\bar{p}$ data. Again, the $0^{-+}(\delta)$ shows an evidence of a resonance peak in the E region, unlike $1^{++}(K^{*})$ and $1^{+-}(K^{*})$.

In summary, we conclude that the D(1285) is largely a 1^{++} state while the E(1420) is predominantly a 0^{-+} state, and both of them require a substantial $\delta\pi$ decay mode. We do not quote at this time the $\delta\pi/K^{*}\bar{K}$ branching ratio for the 0^{-+} E(1420), as its value depends on the precise parametrization of the δ and the $K^{*}(890)$ and is subject to a large systematic error. We should note however that the interference between the two decay modes is substantial with a relatively small statistical error.

In contrast, the 1^{++} $(K^{*}\bar{K})$ wave does not show a resonant behavior at the E mass. Our results, therefore, contradict those of Dionisi, et al.[2] and Armstrong, et al.[18] who find that the E(1420) is a 1^{++} state. On the other hand, our results are clearly in agreement with those of the J/ψ radiative decay,[1,11] and that of Baillon[12], so that the E(1420) and the ι(1440) may very well be the same 0^{-+} object. If the ι(1440) is to be identified as a 0^{-+} glueball, it must be heavily mixed with a $q\bar{q}$ state owing to its prominent production in a hadron-induced reaction such as ours. However, recently measured m = 1458 ± 7 and Γ = 99 ± 6 MeV for the ι(1440) in the J/ψ radiative decay[11] are somewhat higher than those of hadro-produced

E(1420)/ι(1440).

This research was supported by the U.S. Department of Energy under Contract Nos. DE-AC02-76-C00016, DE-AS05-76ER03509, DE-AC02-85ER40125 and by the National Science Foundation Grant #PHY-8120735.

REFERENCES

1. D.L. Sharre, et al., Phys. Lett. B97, 329 (1980);
   C. Edwards, et al., Phys. Rev. Lett. 49, 259 (1982).
2. P. Baillon, et al., Nuovo Cimento 50A, 393 (1967).
3. C. Dionisi, et al., Nuclear Physics B169, 1 (1980).
4. S. Eiseman, et al., Nucl. Instru. Meth. 217, 140 (1983).
5. Ch. Zemach, Phys. Rev. B133, 1201 (1964).
6. S.U. Chung, "Glueball Candidates", presented at XXII Int'l Conf. on HEP, Leipzig, GDR, July 1984.
7. S. Flatte, Phys. Lett. B63, 220 (1976).
   J.B. Gay, et al, Phys. Rev. Lett. 42 346 (1979).
8. S.U. Chung and T.L. Trueman, Phys. Rev. D11, 633 (1975)
9. N.R. Stanton, et al., Phys. Rev. Lett. 42, 346 (1979).
10. T.A. Armstrong, et al., Phys. Lett. B164, 273 (1984).
11. J. Perrier, presented in Physics in Collision, Univ. of California, Santa Cruz, California, August 22-24, 1984.
12. P. Baillon, Proc. of the Seventh Intern. Conf. on Experimental Meson Spectroscopy, Brookhaven National Laboratoy, Upton, NY, April 14-16, 1983. S.J. Lindenbaum, Editor, p. 78 (AIP, New York).

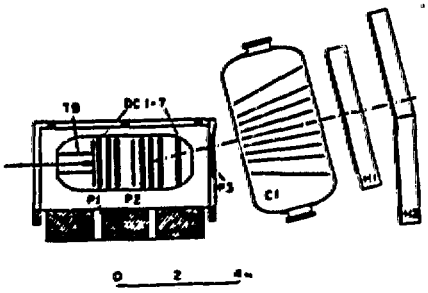

Fig. 1 Schematic diagram of experimental apparatus. Shown at the center is the 30 cm LH_2 target surrounded by a lead-scintillator veto box (TB). P1, P2, P3 are the proportional wire chambers; D.C.'s are the drift-chamber modules; C1 is the high-pressure Cherenkov counter; M1 and M2 are the scintillator-counter hodoscopes.

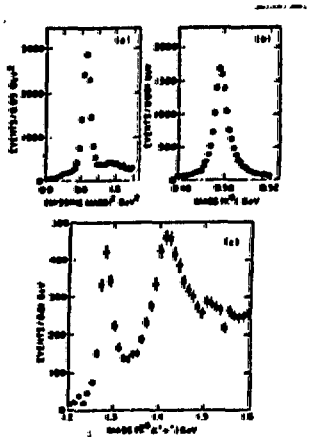

Fig. 2 a) Missing-mass squared (MM^2) spectrum, showing the neutron peak
b) $\pi^+\pi^-$ mass spectrum for the V^0, showing the K^0_S peak
c) $K^+K^0_S\pi^-$ mass spectrum with $0.4 < MM^2 < 1.3$ GeV^2, $0.48 < M(\pi^+\pi^-) < 0.52$ GeV and $t < 1.0$ GeV^2.

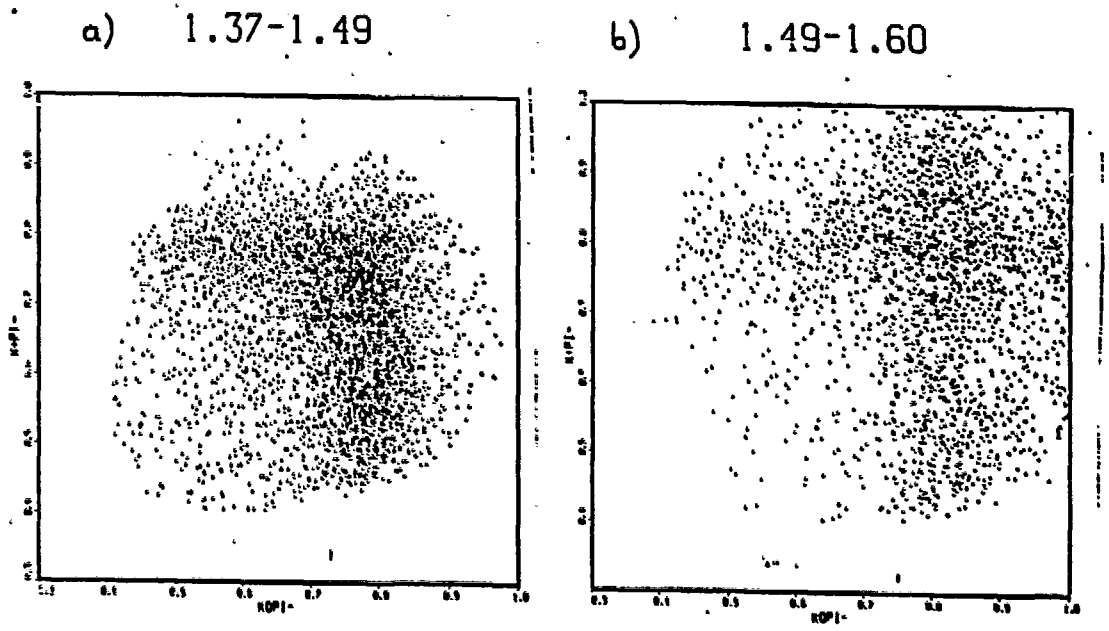

Fig. 3

Dalitz plot distribution for $K^+K^0\pi^-$ system produced in reaction $\pi^-p \to K^+K^0\pi^-n$. The x-axis is $M^2(K^0\pi^-)$, y-axis is $M^2(K^+\pi^-)$.

a) $1.37 < M(K^+K^0\pi^-) < 1.49$ GeV, b) $1.49 < M(K^+K^0\pi^-) < 1.60$ GeV.

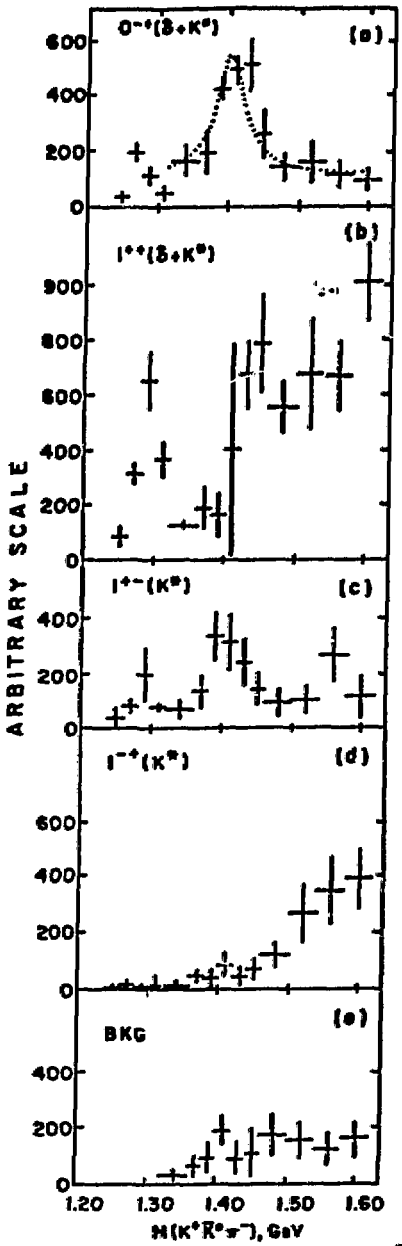

Fig. 4 Acceptance corrected spin-parity content of the (KK+) system (arbitrary scale).
a) $J^{PC} = 0^{-+}$ wave with combined δ+ and K*K̄ decay modes. The dotted curve represents a Breit-Wigner form and a constant background (see text).
b) $J^{PC} = 1^{++}$ wave with combined δ+ and K*K̄ decay modes.
c) $J^{PC} = 1^{+-}$ wave with the K*K̄ decay mode.
d) $J^{PC} = 1^{-+}$ wave with the K*K̄ decay mode
e) Incoherent background.

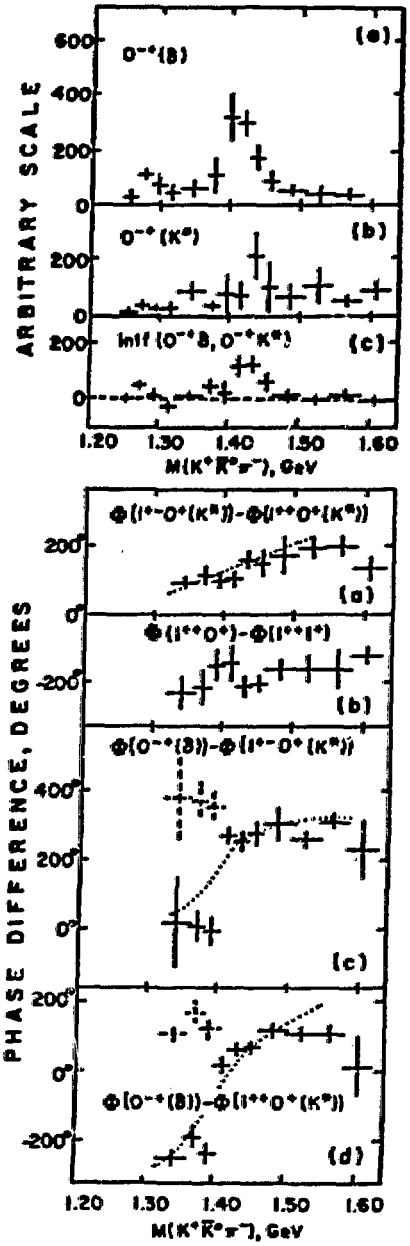

Fig. 5 Contributions to the 0^{-+} wave
a) δ
b) K*K̄
c) Interference term

Fig. 6 Relative phases as functions of KK+ mass
a) $\Phi(1^{+-}0^{+}(K^*)) - \Phi(1^{++}0^{+}(K^*))$
b) $\Phi(1^{++}0^{+}) - \Phi(1^{++}1^{+})$
c) $\Phi(0^{-+}(\delta)) - \Phi(1^{+-}0^{+}(K^*))$
d) $\Phi(0^{-+}(\delta)) - \Phi(1^{++}0^{+}(K^*))$

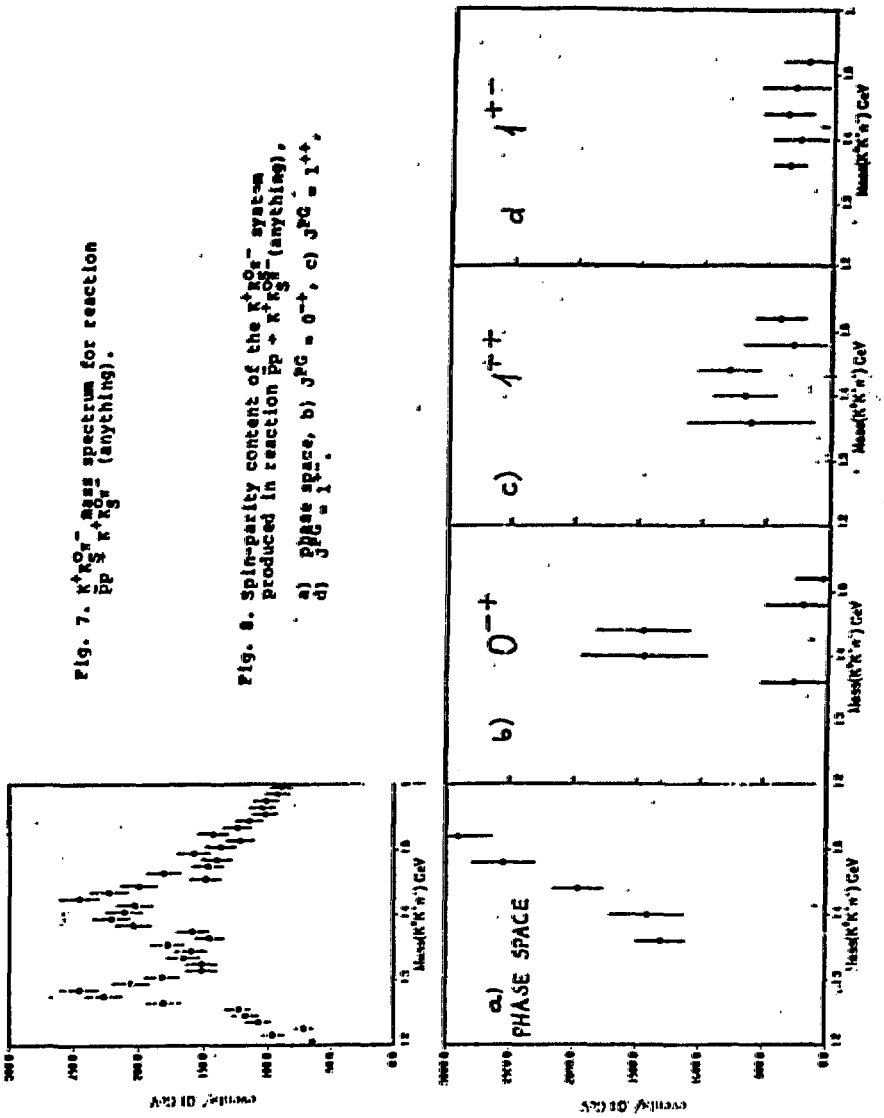

Fig. 7. $K^+K^0_S\pi^-$ mass spectrum for reaction $\bar{p}p \to K^+K^0_S\pi^-$ (anything).

Fig. 8. Spin-parity content of the $K^+K^0_S\pi^-$ system produced in reaction $\bar{p}p \to K^+K^0_S\pi^-$ (anything).
a) phase space, b) $J^{PG} = 0^{-+}$, c) $J^{PG} = 1^{++}$, d) $J^{PG} = 1^{+-}$.

DISCLAIMER

This report was prepared as an account of work sponsored by an agency of the United States Government. Neither the United States Government nor any agency thereof, nor any of their employees, makes any warranty, express or implied, or assumes any legal liability or responsibility for the accuracy, completeness, or usefulness of any information, apparatus, product, or process disclosed, or represents that its use would not infringe privately owned rights. Reference herein to any specific commercial product, process, or service by trade name, trademark, manufacturer, or otherwise does not necessarily constitute or imply its endorsement, recommendation, or favoring by the United States Government or any agency thereof. The views and opinions of authors expressed herein do not necessarily state or reflect those of the United States Government or any agency thereof.